Display Technology Letters

Blue-Phase Liquid Crystals for Reflective Projection Displays

Linghui Rao, Sihui He, and Shin-Tson Wu, *Fellow, IEEE*

***Abstract*—A reflective projection display based on blue phase liquid crystal (BPLC) is proposed. The fast response time of BPLC enables color sequential projection display while suppressing color breakup. Methods for reducing the operation voltage of BPLC are also discussed.**

***Index Terms*—Blue phase liquid crystal (BPLC), reflective projection displays.**

I. Introduction

COLOR sequential projection displays with reflective liquid-crystal-on-silicon (LCoS) require a fast response time. Three operation modes have been commonly used for reflective LCoS projectors: mixed-mode twisted nematic cell [1], vertical alignment nematic (VAN) cell [2], and ferroelectric LC cell [3]. Through thin cell gap approach [4], fast response time can be achieved. However, it is fairly difficult to control the cell gap uniformity when the cell gap is decreased to around 1 μm.

Recently, polymer-stabilized blue phase liquid crystal (BPLC) is emerging for direct-view [5]–[7] and projection [8] displays because of its submillisecond gray-to-gray response time [9], alignment layer free process, and cell gap insensitivity when an in-plane switching (IPS) electrode is used [10], [11].

In this paper, we propose a reflective BPLC IPS cell for color sequential projection displays. To lower the driving voltage, a reflective BPLC cell with patterned electrodes is proposed. In addition, the wavelength dispersion issue is also addressed.

II. Device Structure

Kerr effect is a type of quadratic electro-optic effect caused by an electric-field-induced ordering of polar molecules in an optically isotropic medium. Without an electric field, the BPLC medium appears optically isotropic. As the electric field increases, the isotropic-to-anisotropic transition takes place. The induced birefringence (Δn) can be described by the following extended Kerr effect model [12]:

$$\Delta n = \Delta n_s \left[1 - \exp\left(\frac{E}{E_s}\right)^2\right] \quad (1)$$

Manuscript received July 19, 2012; revised August 07, 2012; accepted August 08, 2012. Date of publication August 31, 2012; date of current version September 07, 2012. This work was supported by ITRI (Taiwan).

The authors are with the College of Optics and Photonics, University of Central Florida, Orlando, FL 32816 USA (e-mail: swu@mail.ucf.edu).

Color versions of one or more of the figures are available online at http://ieeexplore.ieee.org.

Digital Object Identifier 10.1109/JDT.2012.2212875

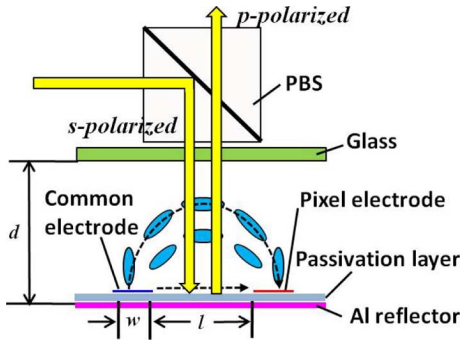

Fig. 1. Basic device structure of the reflective BPLC projection display.

where Δn_s denotes the saturated induced birefringence of the BPLC composite, E is the electric field, and E_s is the saturation field. In the low field region, (1) can be expanded by Taylor series and Kerr constant is expressed as $K = 3\Delta n_s/\lambda(E_s)^2$.

Fig. 1 depicts the proposed reflective projection display with a planar IPS BPLC cell. Here w is the electrode width, l is the spacing between electrodes, and d is the cell gap. Let us assume the polarizing beam splitter (PBS) reflects s-wave and transmits p-wave. In the voltage-off state, the incident s-wave traverses the optically isotropic BPLC layer twice but experiences no phase retardation. Thus, it is blocked by the PBS, leading to a dark state. As the voltage increases, the horizontal fringe fields generated by the IPS electrodes introduce phase retardation to the s-wave. To obtain maximum phase retardation, the polarization of s-wave should be at 45° with respect to the horizontal electric field. As a result, the reflected light from the bottom aluminum (Al) reflector will transmit through the PBS and reach the projection screen. Grayscales can be easily obtained by the applied voltage. However, the embedded Al reflector could distort the horizontal electric fields. To minimize this effect, we added a thin SiO_2 passivation layer on top of the metal. Detail parameters will be described later.

III. Experiment

In experiment, we prepared a BPLC IPS cell (IPS 10–10) with electrode width $w = 10$ μm, electrode gap $l = 10$ μm, and cell gap $d = 7.5$ μm. The BPLC material is JC-BP01M [13]. At ~ 25 °C, we measured the voltage-dependent transmittance (VT) and voltage-dependent reflectance (VR) curves with a He–Ne laser ($\lambda = 633$ nm). The measured results are shown as solid lines in Fig. 2. We used (1) to fit the VT curve (dashed lines) and obtained Kerr constant $K = 10.82$ nm/V^2. With the same Kerr constant, we calculated the VR curve and it fits very well with the experimental data, as depicted in Fig. 2. Compared to the transmissive mode, the reflective mode bares

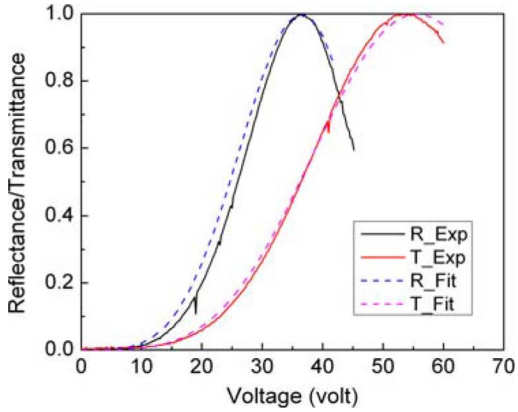

Fig. 2. VT and VR curves of the IPS BPLC cell with $w = 10\ \mu$m, $l = 10\ \mu$m, and $d = 7.5\ \mu$m. Solid lines are experimental results and dashed lines are fitting curves at $\lambda = 633$ nm.

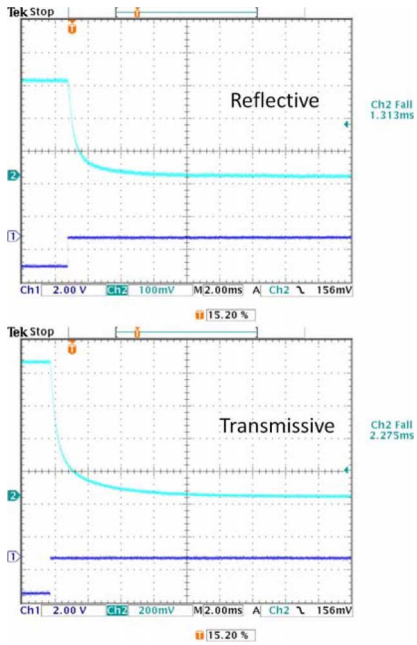

Fig. 3. Measured response time of the IPS 10–10 BPLC cell in reflective mode (upper) and transmissive mode (lower).

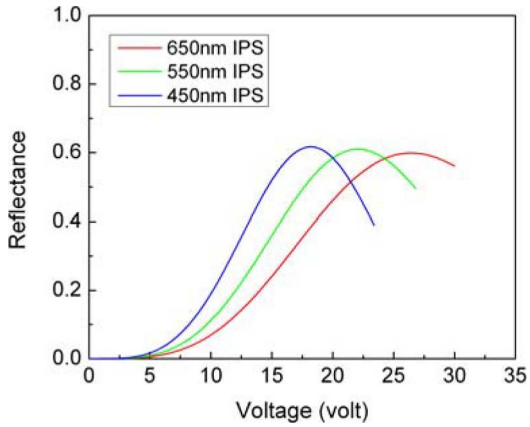

Fig. 4. Simulated VR curves of the reflective BPLC cell with IPS 2–4.

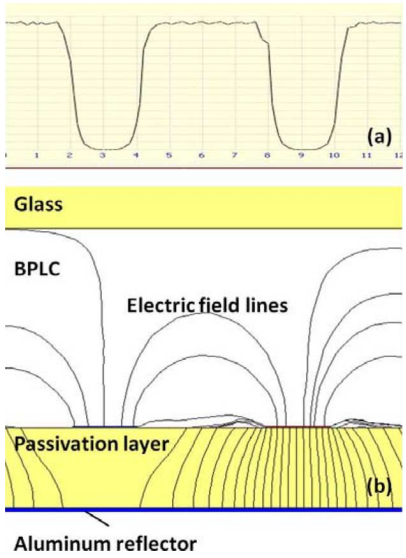

Fig. 5. (a) Reflectance profile and (b) electric field distribution in the reflective IPS BPLCD. Cell: IPS 2–4, $\lambda = 650$ nm, and $V_{\rm on} = 26.4\ V_{\rm rms}$. SiO_2 passivation layer thickness is 1 μm.

a much lower driving voltage as the incident light accumulates twice the phase retardation through double pass. However, with an IPS 10–10 cell, the on-state voltage $(V_{\rm on})$ for the reflective mode is 36 V, which is still too high for LCoS.

We also measured the response time of the reflective BPLC cell. Results are shown in Fig. 3. The decay time is 1.3 ms. For the same BPLC cell, if we measure it in the transmissive mode, the decay time is 2.3 ms. The reason for the faster response time in reflective mode is due to its lower on-state voltage. Response time becomes slower if the applied electric field exceeds a critical field [14] in which lattice distortion or phase transition could take place. If we raise the operating temperature to $\sim 30\ ^\circ$C, the response time is below 1 ms.

IV. Simulation Results and Discussion

To lower the operating voltage, we could decrease the electrode gap so that the electric field is stronger with the same applied voltage. We calculated the reflective IPS BPLCD with electrode width $w = 2\ \mu$m and gap length $l = 4\ \mu$m (IPS 2–4). Depicted in Fig. 4 are the VR curves for red (650 nm), green (550 nm) and blue (450 nm) colors. Compared to 36 V in Fig. 2, the on-state voltage for red color in Fig. 4 is reduced to 26.4 V. Due to wavelength dispersion [7], [15], the $V_{\rm on}$ for 550 nm and 450 nm are 22 V and 18.2 V, respectively.

Fig. 5(a) and (b) depicts simulated reflectance and electric field distributions in the reflective BPLCD (IPS 2–4) with $V_{\rm on} = 26.4\ V_{\rm rms}$ at $\lambda = 650$ nm. As expected, high transmittance occurs in the electrode gap regions. The electric fields on top of the electrodes are in vertical direction so that they do not contribute to the transmittance.

From Fig. 5(b), the lateral fields between the common and pixel electrodes are affected by the aluminum reflector which could potentially decrease the optical efficiency. To reduce electric field distortion, we add a passivation layer, such as SiO_2 or acrylic layer, as Fig. 5(b) shows. A typical passivation layer thickness is $\sim 0.5\ \mu$m to $1.0\ \mu$m, which is sufficient to reduce

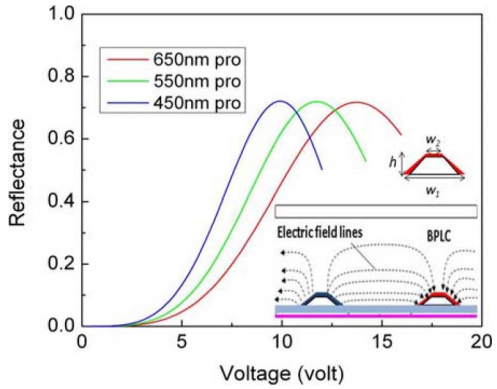

Fig. 6. Simulated VR curves of the reflective BPLC cell with protrusion electrodes at the specified wavelengths. Inset is the structure of the reflective BPLCD with protruded electrodes.

the electric field bending effect. From our simulation, the optical efficiency with such a passivation layer is only $\sim 5\%$ lower than that of the ideal case.

To further decrease the operating voltage, protruded electrodes can be employed [16]. Fig. 6 shows the simulated VR curves of the reflective BPLC cell with protrusion electrodes at RGB wavelengths. Inset is the structure of the protrusion electrodes. The dimension of the trapezoid electrode structure is defined as follows: w_1 is the bottom width, w_2 is the top width, h is the height, and l is the space between the electrodes. In this simulation, $w_1 = 2\ \mu$m, $w_2 = 1\ \mu$m, $h = 2\ \mu$m, and $l = 4\ \mu$m. With the protruded electrodes, the electric field is stronger and it penetrates deeper into the BPLC bulk region. Therefore, the on-state voltages for the RGB colors are decreased to 13.8, 11.8, and 10 V, respectively.

From Figs. 4 and 6, we can see that the wavelength dispersion of the VR curves is quite different from that of a nematic IPS cell, although we also use IPS electrodes for our BPLC. The reasons are explained as follows. In a nematic IPS cell, both top and bottom substrates have strong anchoring energy originated from rubbing. At a given voltage, the electric field strength decreases gradually from the bottom substrate (IPS electrodes) to the top. As a result, double TN cells with reversed twists are formed [17]. Due to polarization rotation effect, the TN cells are inert to the wavelength [18]. However, in a BPLC cell, there is no surface rubbing. And moreover, the Kerr constant of a BPLC material is related to the wavelength as [7], [15]

$$\lambda K = G\frac{\lambda^2\lambda^{*2}}{\lambda^2 - \lambda^{*2}} \tag{2}$$

here λ^* is the mean resonance wavelength and G is a proportionality constant. Therefore, the VT/VR curves of an IPS-based BPLC are similar to those of a VAN cell.

Also noticed from Fig. 6, the peak reflectance of the BPLC cell is only 72%. This is because of the dead zones above the IPS electrodes, as Fig. 5(a) shows. However, in experiment the transmittance could reach 85%–90% because of the dielectric coupling effect [19]. This dielectric coupling effect helps to reorient the BPLC near the electrode edges so that the effective aperture ratio is increased. A tradeoff is in the slightly higher voltage. This optical efficiency is comparable to that of VAN mode after having considered the fringing field effect [20].

V. Conclusion

We proposed a color-sequential projection display using reflective mode polymer-stabilized BPLCD. The fast response time of BPLC enables color-sequential technique to be implemented for LCD projector. The alignment-layer-free feature of BPLC simplifies the fabrication process.

Acknowledgment

The UCF group is indebted to Dr. Y. Haseba of JNC for providing the BPLC material.

References

[1] S. T. Wu and C. S. Wu, "Mixed mode twisted nematic liquid crystal cells for relective displays," *Appl. Phys. Lett.*, vol. 68, pp. 1455–1457, 1996.
[2] H. D. Smet, D. Cuypers, A. V. Calster, J. V. Steen, and G. V. Doorselaer, "Design, fabrication and evaluation of a high-performance XGA VAN-LCOS microdisplay," *Displays*, vol. 23, pp. 89–98, 2002.
[3] S. Lee, C. Mao, and K. M. Johnson, "Fast-switching liquid- crystal-on-silicon microdisplay with frame buffer pixels and surface mode optically compensated birefringence," *Opt. Eng.*, vol. 45, p. 127402, 2006.
[4] S. Gauza, X. Zhu, W. Piecek, R. Dabrowski, and S. T. Wu, "Fast switching liquid crystals for color-sequential LCDs," *J. Display Technol.*, vol. 3, no. 3, pp. 250–252, Sep. 2007.
[5] H. Kikuchi, M. Yokota, Y. Hiskado, H. Yang, and T. Kajiyama, "Polymer-stabilized liquid crystal blue phases," *Nat. Mater.*, vol. 1, pp. 64–68, 2002.
[6] Z. Ge, S. Gauza, M. Jiao, H. Xianyu, and S. T. Wu, "Electro-optics of polymer-stabilized blue phase liquid crystal displays," *Appl. Phys. Lett.*, vol. 94, p. 101104, 2009.
[7] Z. Ge, L. Rao, S. Gauza, and S. T. Wu, "Modeling of blue phase liquid crystal displays," *J. Display Technol.*, vol. 5, no. 7, pp. 250–256, Jul. 2009.
[8] S. He, J. H. Lee, H. C. Cheng, J. Yan, and S. T. Wu, "Fast-response blue-phase liquid crystal for color sequential displays," *J. Display Technol.*, vol. 8, no. 6, pp. 352–356, Jun. 2012.
[9] K. M. Chen, S. Gauza, H. Xianyu, and S. T. Wu, "Submillisecond gray-level response time of a polymer-stabilized blue-phase liquid crystal," *J. Display Technol.*, vol. 6, no. 2, pp. 49–51, Feb. 2010.
[10] L. Rao, J. Yan, and S. T. Wu, "Prospects of emerging polymer-stabilized blue-phase liquid crystal displays," *J. Soc. Inf. Disp.*, vol. 18, pp. 954–959, 2010.
[11] L. Rao, Z. Ge, S. Gauza, K. M. Chen, and S. T. Wu, "Emerging liquid crystal displays based on the Kerr effect," *Mol. Cryst. Liq. Cryst.*, vol. 526, pp. 185–197, 2010.
[12] J. Yan, H. C. Cheng, S. Gauza, Y. Li, M. Jiao, L. Rao, and S. T. Wu, "Extended Kerr effect in polymer-stabilized blue-phase liquid crystals," *Appl. Phys. Lett.*, vol. 96, p. 071105, 2010.
[13] L. Rao, J. Yan, and S. T. Wu, "A large Kerr constant polymer-stabilized blue phase liquid crystal," *Appl. Phys. Lett.*, vol. 98, p. 081109, 2011.
[14] J. Yan, Y. Chen, S. T. Wu, S. H. Liu, and K. L. Cheng, "Dynamic response of a polymer-stabilized blue-phase liquid crystal," *J. Appl. Phys.*, vol. 111, p. 063103, 2012.
[15] M. Jiao, J. Yan, and S. T. Wu, "Dispersion relation on the Kerr constant of a polymer-stabilized optically isotropic liquid crystal," *Phys. Rev. E.*, vol. 83, p. 041706, 2011.
[16] L. Rao, Z. Ge, S. T. Wu, and S. H. Lee, "Low voltage blue-phase liquid crystal displays," *Appl. Phys. Lett.*, vol. 95, p. 231101, 2009.
[17] Z. Ge, S. T. Wu, S. S. Kim, J. W. Park, and S. H. Lee, "Thin cell fringe-field-switching liquid crystal display with a chiral dopant," *Appl. Phys. Lett.*, vol. 92, p. 181109, 2008.
[18] M. Schadt and W. Helfrich, "Voltage-dependent optical activity of a twisted nematic liquid crystal," *Appl. Phys. Lett.*, vol. 18, pp. 127–128, 1971.
[19] K. M. Chen, J. Yan, S. T. Wu, Y. P. Chang, C. C. Tsai, and J. W. Shiu, "Electrode dimension effects on blue-phase liquid crystal displays," *J. Display Technol.*, vol. 7, no. 7, pp. 362–364, Jul. 2011.
[20] K. H. Fan-Chiang, S. T. Wu, and S. H. Chen, "Fringing-field effects on high-resolution liquid crystal microdisplays," *J. Display Technol.*, vol. 1, no. 2, pp. 304–313, Dec. 2005.